AD-A114 927 NEW MEXICO STATE UNIV LAS CRUCES DEPT OF ELECTRICAL --ETC F/6 20/5
OPTIMAL CONTROL OF THE HEL BEAM.(U)
FEB 82 J E STEELMAN AFOSR-81-0081
UNCLASSIFIED AFOSR-TR-82-0387 NL

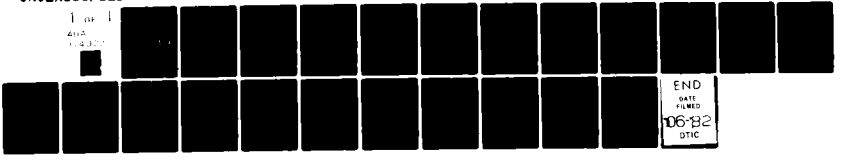

END
DATE FILMED
06-82
DTIC

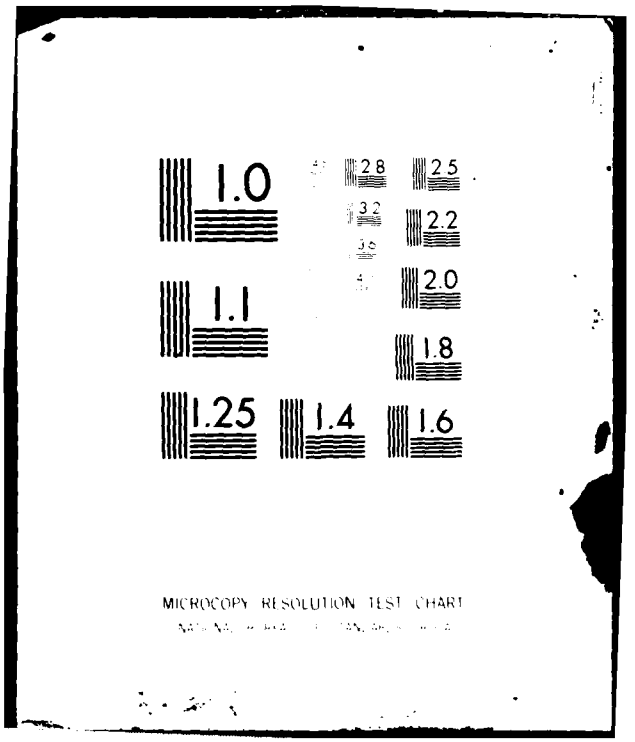
1.0
2.8
2.5
3.2
2.2
3.6
4
2.0
1.1
1.8
1.25
1.4
1.6
MICROCOPY RESOLUTION TEST CHART

UNCLASSIFIED

SECURITY CLASSIFICATION OF THIS PAGE (When Data Entered)

REPORT DOCUMENTATION PAGE	READ INSTRUCTIONS BEFORE COMPLETING FORM
1. REPORT NUMBER **AFOSR-TR- 82-0387** 2. GOVT ACCESSION NO. AD-A11492 7	3. RECIPIENT'S CATALOG NUMBER
4. TITLE (and Subtitle) OPTIMAL CONTROL OF THE HEL BEAM	5. TYPE OF REPORT & PERIOD COVERED Final Report 1 Feb 81 - 31 Jan 82
	6. PERFORMING ORG. REPORT NUMBER
7. AUTHOR(s) J. Eldon Steelman	8. CONTRACT OR GRANT NUMBER(s) AFOSR-81-0081
9. PERFORMING ORGANIZATION NAME AND ADDRESS Electrical and Computer Engineering New Mexico State University Las Cruces, New Mexico 88003	10. PROGRAM ELEMENT, PROJECT, TASK AREA & WORK UNIT NUMBERS 61102F 2301-D9
11. CONTROLLING OFFICE NAME AND ADDRESS AFOSR/NP Bolling AFB, DC 20332	12. REPORT DATE February 1982
	13. NUMBER OF PAGES 20
14. MONITORING AGENCY NAME & ADDRESS(if different from Controlling Office)	15. SECURITY CLASS. (of this report) Unclassified
	15a. DECLASSIFICATION DOWNGRADING SCHEDULE

16. DISTRIBUTION STATEMENT (of this Report)

Approved for public release: Distribution Unlimited

DTIC ELECTE MAY 25 1982 S D B

17. DISTRIBUTION STATEMENT (of the abstract entered in Block 20, if different from Report)

18. SUPPLEMENTARY NOTES

19. KEY WORDS (Continue on reverse side if necessary and identify by block number)

High Energy Laser, Atmospheric Turbulence Effects, Optimal Control

20. ABSTRACT (Continue on reverse side if necessary and identify by block number)

Optimal control of the deformable mirror in a High Energy Laser was used to reduce the effects of atmospheric turbulence. The performance characteristics of an optical detector with one or four sub-apertures were estimated. These estimated performance characteristics were then used to determine the regime where four sub-apertures gave better performance than one sub-aperture for no time delay and for a one millisecond time delay.

DD FORM 1 JAN 73 1473

UNCLASSIFIED

SECURITY CLASSIFICATION OF THIS PAGE (When Data Entered)

ACKNOWLEDGEMENTS

The author would like to thank the Air Force Systems Command, the Air Force Office of Scientific Research, and the Southeastern Center for Electrical Engineering Education for sponsoring this research. He would also like to express his appreciation to Capt. Hal McIntire, Mrs. Pat Simari, Dr. Arnold Elsbernd, Mr. Don Evey, and Miss Dion Messer for providing computer assistance. The author would also like to thank Ms. Dolores Mendoza for typing this report. Further, he would like to thank Dr. Frank Carden for supporting this research effort in many different ways.

The author would like to thank Col. James A. Dillow for suggesting this area of research and for his guidance. Dr. Russ Butts, Maj. Charles Corsetti, and Capt. Charles Martin have also provided much useful information and many helpful suggestions.

AFOSR-81-0081

OPTIMAL CONTROL OF THE HEL BEAM

BY

J. Eldon Steelman

ABSTRACT

Optimal control of the deformable mirror in a High Energy Laser was used to reduce the effects of atmospheric turbulence. The performance characteristics of an optical detector with one or four sub-apertures were estimated. These estimated performance characteristics were then used to determine the regime where four sub-apertures gave better performance than one sub-aperture for no time delay and for a one millisecond time delay.

I. INTRODUCTION:

Optimal control of the deformable mirror in a High Energy Laser (HEL) (see Figure 1) is used to offset the turbulence in the atmosphere. This research effort seeks the best control system for the HEL as a function of the measurement statistics and the number of detector sub-apertures. The number of sub-apertures is important because more sub-apertures allow the estimation of higher order optical effects and the potential for better control. However, increasing the number of sub-aperture increases the measurement variance.

The primary tool used in this determination was computer modeling. Kleinman's routines (References 1 through 5) were used to determine the optimal continuous control and the steady-state gain of a continuous Kalman estimator. Kleinman's routines were also used to find the overall system covariance matrix.

II. OBJECTIVES OF THE RESEARCH EFFORT:

The objective of this project was to determine the system for the deformable mirror which minimized the effects of atmospheric turbulence. The reduction in atmospheric turbulence effects was found as a function of measurement statistics and number of sub-apertures. The reduction was found for the first five optical modes with time delays of 0 and 1 msec. A basic assumption was that each optical mode could be estimated separately and linearly.

III. ATMOSPHERIC TURBULENCE:

The distortion induced in the laser beam by atmospheric turbulence can be described in terms of its effect on the various optical modes (tilt, focus, astigmatism, etc.). The effect on each optical mode can be modeled by a three state variable model driven by a Gaussian random variable (References 6 and 7).

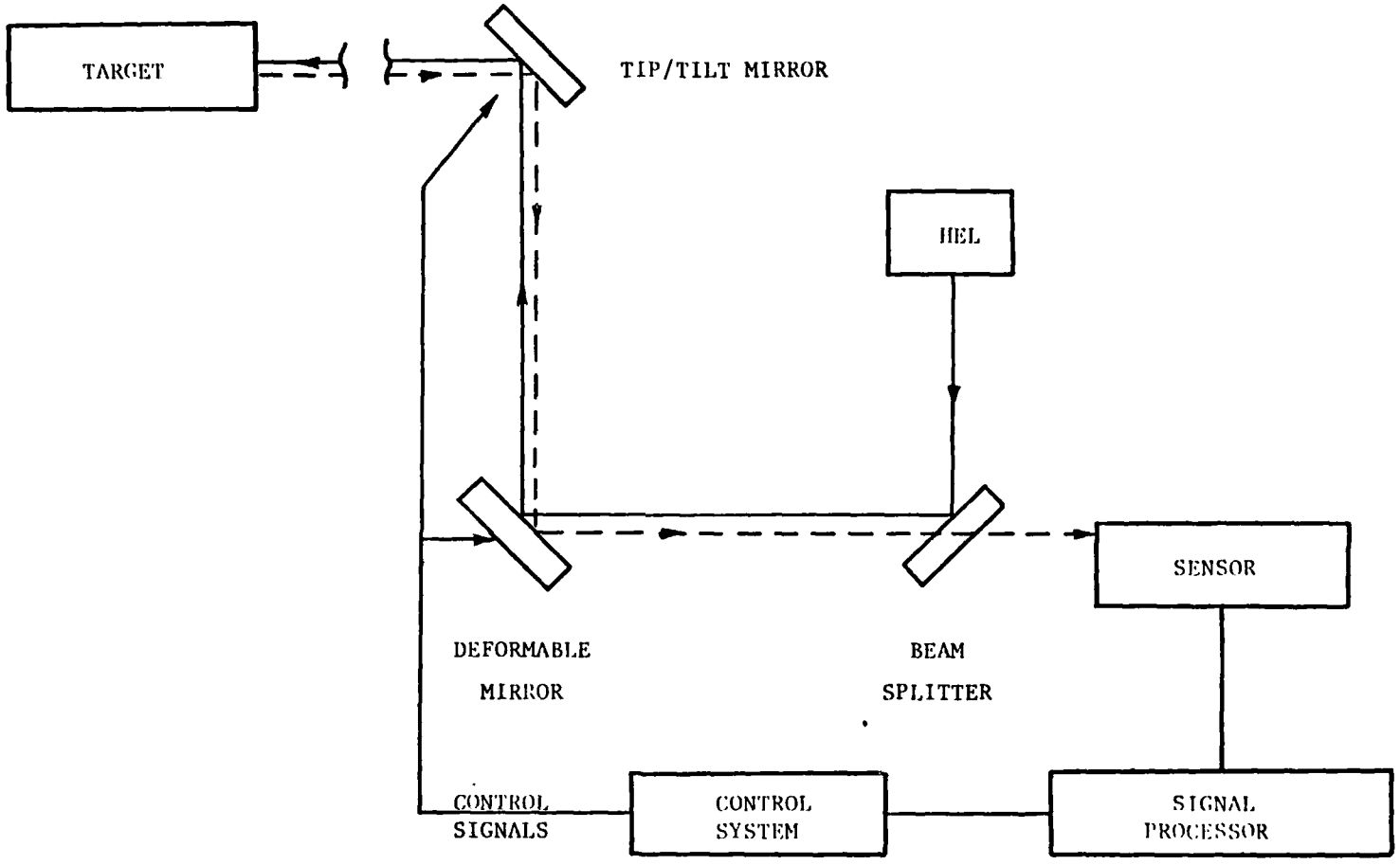

Figure 1. Simplified HEL Control System

Let $x_1 = v_x$ = random effect on optical mode

x_2 = turbulence model state

x_3 = turbulence model state

Then the state model is

$$\dot{x}_1 = -a x_1 + a x_2 \quad (1)$$

$$\dot{x}_2 = -b x_2 + b x_3 \quad (2)$$

$$\dot{x}_3 = -c x_3 + v_t \quad (3)$$

where v_t is white noise with covariance

$$E\{v_t(t)\, v_t(t+T)\} = k\delta(T) \quad (4)$$

Values of k, a, b, and c for the first five optical modes are given in Table I (Reference 7).

Table I. Parameters for Turbulence Model

Mode	Name	k	a	b	c
x	Tilt	2.6×10^{-7}	47.10	2200	2200
y	Tip	2.4×10^{-7}	47.10	2200	2200
$x^2 + y^2 - R^2/2$	Focus	3.3×10^{-8}	94.20	3350	3350
$x^2 - y^2$	Astig-1	5.4×10^{-8}	41.80	2576	2576
xy (exact)	Astig-2	6.0×10^{-10}	4.710	73.30	2932
xy (approx.)		5.65×10^{-6}	73.30	2932	3×10^4

NOTE: Mode xy (exact) has a zero at .0523 radians/sec

The steady-state output covariance of the system described by equations (1) through (4) may be found by solving the linear variance equation (reference 9)

$$A X + A^T X + Q = 0 \quad (5)$$

where

A is the 3 by 3 system matrix from equations 1 through 3

Q is a 3 by 3 matrix with $q_{33} = k$ the only non-zero term

X is the covariance matrix of $[x_1\ x_2\ x_3]^T$

The resultant entries of x are

$$x_{11} = x_{12} = x_{21} = \frac{ab(a+b+c)k}{2(a+b)(a+c)(b+c)c} \tag{6}$$

$$x_{13} = x_{31} = \frac{ab\ k}{2(bc)(a+c)c} \tag{7}$$

$$x_{22} = x_{23} = x_{32} = \frac{b\ k}{2(b+c)\ c} \tag{8}$$

$$x_{33} = \frac{k}{2c} \tag{9}$$

To avoid a special program for mode xy (astigmatism-2), mode xy was modelled by the approximate model shown as the last line of Table I. This approximate model resulted from two approximations. First, the zero at .0523 was cancelled by the pole at 4.71. (This cancellation multiplied k by 4.71/.0523). Secondly, the linear variance equation for the resulting 2 pole system was solved to yield

$$x'_{11} = \frac{a\ k'}{2(a+b)b} \tag{10}$$

Finally, an effective k was chosen so that the variance of x_1 from (6) and the variance from (10) were identical when a remote third pole ($c \cong 10b$) was included.

The effect of atmospheric turbulence upon the intensity at the target is a function of Zernike residual errors (reference 11 and 13). These residual errors and differences are tabulated in Table II.

Table II. Zernike Residual Errors and Strengths

Mode	$\Delta_i (=\sigma_i^2)$	Difference (Strength of aberration)
	1.03	
Tilt		.448
	0.582	
Tip		.448
	0.134	
Focus		.023
	0.111	
Astig-1		.023
	0.088	
Astig-2		.023
	.065	

NOTE: All quantities must be multiplied by $(D/r_o)^{5/3}$

The normalized, on-axis for field irradiance, I_{rel}, is usually found from the Strehl approximation

$$I_{rel} = \exp(-\sigma^2)$$

The Strehl approximation is not valid for large values of σ^2. Thus, the figure of merit used in this research effort is the normalized phase variance σ^2/σ_o^2 where $\sigma_o^2 = 1.03\,(D/r_o)^{5/3}$. For example, if tilt and tip could be completely corrected (or removed) the normalized variance would be 0.134/1.03.

IV. MIRROR AND CONTROL SYSTEM MODEL:

The mirror tilt and control system are represented by three state variables.

Let x_4 = mirror tilt (11)

x_5 = mirror tilt rate (12)

x_6 = integral of error $(x_1 - x_4)$ (13)

Finally, the mirror drive is a force driver such that

$$\dot{x}_4 = x_5 = u \tag{14}$$

The complete tilt system model is

$$\begin{bmatrix} \dot{x}_1 \\ \dot{x}_2 \\ \dot{x}_3 \\ \dot{x}_4 \\ \dot{x}_5 \\ \dot{x}_6 \end{bmatrix} = \begin{bmatrix} -a & a & 0 & 0 & 0 & 0 \\ 0 & -b & b & 0 & 0 & 0 \\ 0 & 0 & -c & 0 & 0 & 0 \\ 0 & 0 & 0 & 0 & 1 & 0 \\ 0 & 0 & 0 & 0 & 0 & 0 \\ 1 & 0 & 0 & -1 & 0 & 0 \end{bmatrix} \begin{bmatrix} x_1 \\ x_2 \\ x_3 \\ x_4 \\ x_5 \\ x_6 \end{bmatrix} + \begin{bmatrix} 0 \\ 0 \\ 0 \\ 0 \\ 1 \\ 0 \end{bmatrix} u + \begin{bmatrix} 0 \\ 0 \\ v_t \\ 0 \\ 0 \\ 0 \end{bmatrix} \tag{15}$$

The covariance matrix for the driving noise is all zeros except for

$$q_{33} = k \tag{16}$$

The remaining four optical modes will be modeled by the same general equation. The different values from Table I will be used in equations (15) and (16).

V. SYSTEM OBSERVATION MATRIX:

The observation system will be represented by $\underline{y} = M\,\underline{x} + \underline{v}_m$. The quantity y_1 is measured by the detector.

$$y_1 = x_1 - x_4 + v_1 \tag{17}$$

Observability requires that x_6 also be measured

$$y_3 = x_6 + v_3 \tag{18}$$

The programs developed for the research (reference 14) also permitted the measurement of x_4

$$y_2 = x_4 + v_2 \tag{19}$$

However, a knowledge of x_4 did not improve the system performance and the coefficients associated with this measurement were later set to zero.

VI. OPTIMAL CONTROL SYSTEM DESIGN:

The classical infinite time optimal control problem minimizes a cost function (Reference 8).

$$V = \int_o^\infty (x^t Q_1 x + u^t R_1 u)\, dt \tag{20}$$

The minimization of V produces the control in terms of P_1, the solution to a Ricatti equation

$$P_1 A + A^t P_1 - P_1 \underline{b} R_1^{-1} \underline{b}^t P_1 + Q_1 = 0 \tag{21}$$

(Kleinman's subroutine MRIC solves this equation.)

The optimal control is

$$\underline{u}^* = - R_1^{-1} \underline{b}^t P_1 \tag{22}$$

The optimal control can be required to have a prescribed stability by replacing A by $(\alpha U + A)$.

VII. KALMAN STATE ESTIMATOR:

If the basic plant is described by (reference 8)

$$\dot{\underline{x}} = A \underline{x} + B \underline{u} + \underline{v}_x \tag{23}$$

$$\underline{y} = M \underline{x} + \underline{v}_m \tag{24}$$

The Kalman estimator is

$$\underline{x}_e = A \underline{x}_e + B \underline{u} + k_e (M \underline{x}_e - \underline{y}) \tag{25}$$

Desired control law

$$\underline{u} = L \underline{x} \tag{26}$$

Actual control law

$$\underline{u} = L \underline{x}_e \tag{27}$$

Defining

$$\underline{e} = \underline{x} - \underline{x}_e \tag{28}$$

yields a new system with doubled dimension

$$\begin{bmatrix} \dot{\underline{x}} \\ \dot{\underline{e}} \end{bmatrix} = \begin{bmatrix} A + B L & -B L \\ 0 & A + k_e M \end{bmatrix} \begin{bmatrix} \underline{x} \\ \underline{e} \end{bmatrix} + \begin{bmatrix} \underline{v}_x \\ \underline{v}_x + k_e \underline{v}_m \end{bmatrix} \tag{29}$$

The matrix k_e is the Kalman gain. It is given by

$$k_e = - P_2 M^t R_m^{-1} \tag{30}$$

where k_m is the covariance of $\underline{v}_m$.

P_2 (the covariance of $\underline{e}$) is the solution to (Reference 8)

$$P_2 A^t + A P_2 - P_2 M^t R_m^{-1} M P_2 + Q_n = 0 \tag{31}$$

Q_n is the covariance of $\underline{v}_x$.

R_m is the covariance of $\underline{v}_m$.

The input covariance for equation (29) is

$$\text{cov} \begin{bmatrix} \underline{v}_x \\ \underline{v}_x + k_e \underline{v}_m \end{bmatrix} = E \begin{bmatrix} \underline{v}_x & \underline{v}_x^t & \underline{v}_x^t + \underline{v}_m^t k_e^t \\ \underline{v}_x + k_e \underline{v}_m & & \end{bmatrix}$$

Thus,

$$\text{cov} \begin{bmatrix} \underline{v}_x \\ \underline{v}_x + k_e \underline{v}_m \end{bmatrix} = \begin{bmatrix} Q_n & Q_n \\ Q_n & Q_n + k_e R_m k_e^t \end{bmatrix} = Q_{12} \tag{32}$$

The (2,2) term can be further simplified by substituting equation (30).

$$k_e R_m k_e^t = P_2 M^t R_m^{-1} R_m (R_m^{-1})^t M P_2$$
$$= P_2 (M^t R_m^{-1} M) P_2$$

Thus, the (2,2) term becomes

$$Q_n + k_e R_m k_e^t = Q_n + P_2 (M^t R_m^{-1} M) P_2 \tag{33}$$

The steady-state output covariance for the double dimension system described by equation (29) is the solution of the linear variance equation

$$A_{12} P_{12} + P_{12} A_{12}^t + Q_{12} = 0 \tag{34}$$

where P_{12} is the covariance of $[\underline{x}^t \ \underline{e}^t]$

A_{12} is the double dimension system matrix

Q_{12} is the input covariance from (32)

Kleinman (reference 10) modified the system described above by including the effects of time delay in the observation system.

$$\underline{y}(t) = M \underline{x}(t - T) + \underline{v}_m (t - T) \tag{35}$$

Given this observation model Kleinman obtains the following expression for the covariance of $\underline{x}$.

$$P_x = e^{AT} P_2 e^{A^t T} + \int_0^T e^{At} P_2 M^t R_m^{-1} M P_2 e^{A^t t} \, dt$$

$$+ \int_0^\infty e^{\bar{A}t} e^{AT} P_2 M^t R_m^{-1} M e^{A^t T} e^{\bar{A}^t t} \, dt \tag{36}$$

where $\bar{A} = A + BL$ (term from (29))

(Kleinman's routine INTEG performs numerical integrations of this type).

VIII DETECTOR MODELS:

Martin (reference 11) presents this result for the variance of an upgraded shearing interferometer measurement

$$\sigma^2_{SI} = \frac{\frac{\pi^2}{2} M^2 C^2_{det} \left(\frac{\alpha_d \alpha_{FOV}}{\alpha_o}\right)^2 \left[1 + \left(\frac{\alpha_d}{\alpha_o}\right)^2\right]}{\sin^2\left[\pi \frac{\alpha_o}{\alpha_{FOV}} \left(1 + \left(\frac{\alpha_d}{\alpha_o}\right)^2\right)^{1/2}\right]} \tag{37}$$

where $C_{DET} = 4.17 \times 10^{-4}$

M^2 = number of sub-apertures

$\alpha_d = 4 \times 10^{-6}$ radians

$\alpha_{FOV} = 2 \times 10^{-5} M$

α_o is shown in Table III.

Substituting values into equation (37) produces

$$\sigma_{SI}^2 = \frac{M^2 f}{\sin^2[g/M]} \tag{38}$$

With f and g from Table III equation (38) yields the results also shown in Table III.

Table III. Values and Results for Detector Calculations

	Small Target	Medium Target	Large Target
		VALUES	
α_o (SR)	10^{-12}	10^{-11}	10^{-10}
α_o (radians)	1.13×10^{-6}	3.57×10^{-6}	1.13×10^{-5}
f	2.42×10^{-7}	3.11×10^{-8}	6.96×10^{-9}
g	.653	.842	1.88
		Results (σ_{si}-radians x 10^{-8})	
M = 1	39.8	4.17	0.731
M = 2	301.	30.5	3.45
M = $\sqrt{12}$	1549	155.	16.2

In all cases the aperture was modeled as a circular device. However, the four sub-aperture case (M = 2) and the 12 sub-aperture case (M = $\sqrt{12}$) assumed that the circular aperture was subdivided into square sub-apertures.

The results from Table III were used directly for v_1 in the single aperture case.

Now each detector can measure only tilt (mode x) and tip (mode y). Thus, higher order modes must be estimated from tilt and tip measurements made at the various sub-apertures. Furthe, if all the sub-aperture measurements have the same noise behavior, then a least square estimate is also a minimum variance estimate. This linear estimation procedure was derived by seeking the sub-aperture measurements in terms of the first five modes (reference 12). The following measurement model was used.

$$\underline{m} = H\,\underline{a} + \underline{v}'_m \tag{39}$$

where

$$\underline{m} = \begin{bmatrix} \text{tilt(1)} \\ \text{tilt(2)} \\ \text{tilt(3)} \\ \text{tilt(4)} \\ \text{tip(1)} \\ \text{tip(2)} \\ \text{tip(3)} \\ \text{tip(4)} \end{bmatrix} \quad \text{and} \quad \underline{a} = \begin{bmatrix} \text{overall tilt} \\ \text{overall tip} \\ \text{focus} \\ \text{astig-1} \\ \text{astig-2} \end{bmatrix}$$

$\underline{v}_m$ = sub-aperture noise vector

$\underline{m}$ = measurements at each sub-aperture

$\underline{a}$ = optical modes into the aperture

The expressions for $H_{i,j}$ are

$$H_{i,j} = \frac{1}{A_i} \iint_{A_i} \frac{\partial Z_j}{\partial x}\, dA, \quad 1 \le i \le 4 \tag{40}$$

and

$$H_{i,j} = \frac{1}{A_i} \iint_{A_i} \frac{\partial Z_j}{\partial j}\, dA, \quad 4 \le i \le 8 \tag{41}$$

where Z_j = mode j as a function of x and y. For a circle divided into four 90° segments, the H matrix is

$$H = \begin{bmatrix} 1 & 0 & 2k & k & k \\ 1 & 0 & -2k & -k & k \\ 1 & 0 & -2k & -k & -k \\ 1 & 0 & 2k & k & -k \\ 0 & 1 & 2k & -k & k \\ 0 & 1 & 2k & -k & -k \\ 0 & 1 & -2k & k & -k \\ 0 & 1 & -2k & k & k \end{bmatrix} \tag{42}$$

where $k = 8/3\pi$

Finally, the least square estimates are obtained from the sub-aperture measurements of tip and tilt by

$$\underline{a}_e = (H^t H)^{-1} H^t \underline{m} \tag{43}$$

The covariance of the least square estimates is (for four identical detectors)

$$s = \sigma^2 (H^t H)^{-1} \tag{44}$$

Thus, the variances for the estimations are

$$\sigma^2 \text{ (tilt)} = \sigma_i^2/4 \tag{45}$$

$$\sigma^2 \text{ (tip)} = \sigma_i^2/4 \tag{46}$$

$$\sigma^2 \text{ (focus)} = \sigma_i^2/32k^2) \tag{47}$$

$$\sigma^2 \text{ (astig-1)} = \sigma_i^2/(8k^2) \tag{48}$$

$$\sigma^2 \text{ (astig-2)} = \sigma_i^2/(8k^2) \tag{49}$$

where σ_i^2 = variance of tilt and tip for each detector. The resulting sigmas for each mode and the various target sizes are shown in Table IV.

Table IV. Sigma (x 10^{-8}) in Radians

	Small Target	Medium Target	Large Target
σ(tilt)	151	15.2	1.73
σ(tip)	151	15.2	1.73
σ(focus)	62.8	6.34	.718
σ(astig-1)	126.	12.7	1.44
σ(astig-2)	126.	12.7	1.44

IX. RESULTS AND CONCLUSIONS:

Optimal Control Results

The Q_1 and R_1 matrices of equation 20 and alpha of equation 22 were selected to produce a closed loop system with a damped natural frequency of about 500 Hz and a damping ratio of about 0.707. The values used and the resulting three controllable eigenvalues are shown in Table V.

Table V. Values and Results for Optimal Control

	Tilt (& Tip)	Focus	Astig-1	Astig-2*
$Q_1(1,1)$	$.145 \times 10^{10}$	$.2 \times 10^{9}$	$.145 \times 10^{10}$	$.13 \times 10^{10}$
$Q_1(5,5)$	121	95.5	121	119
$Q_1(6,6)$	$.139 \times 10^{17}$	$.89 \times 10^{16}$	$.139 \times 10^{17}$	$.135 \times 10^{10}$
R_1^{-1}	$.125 \times 10^{6}$	$.6 \times 10^{6}$	$.125 \times 10^{6}$	$.143 \times 10^{6}$
Alpha	45	90	40	21.1
Real Eigenvalue	-4383	-7825	-4367	-4460
Complex	-2215	-2220	-2215	-2222
Eigenvalues	±j2218	±j2220	±j2218	±j2218

NOTE: $Q_1(4,4) = Q_1(1,1) = -Q_1(1,4), -Q_1(4,1)$

Eigenvalues in per second

*For approximate 3 pole model

Kalman Filter Results

The steady-state Kalman filter was used to estimate the states of the turbulence model. As discussed in Section V observability requires that state x_6 (the integral of $x_1 - x_4$) be measured. So, in lieu of attempting to establish one sigma for x_6, the sigma for x_6 was varied. The computer programs presented in reference 14 were modified slightly to solve the expression of equation (36) and to calculate a variance reduction ratio for each set of input data.

The results of this research are shown in the graphs of Figures 2 through 7. The graphs of Figures 2 thorugh 4 present the results for one and four sub-apertures and for the three different target sizes with no time delay. The graphs of Figures 5 through 7 present the same results for a time delay of one millisecond.

These graphs reveal that if the variance of the integral of the error is small enough, then four sub-apertures provide a smaller normalized phase variance than does a single aperture.

Optical Detector Assumptions

1. $C_{DET} = 4.17 \times 10^{-4}$
2. A quarter circle can be modeled by a square with the same area. (assumed for the four sub-aperture case)

Control System Assumptions

1. The mirror dynamics permit a damped natural frequency of 500 Hz with a damping factor of 0.707.
2. The modes are not coupled.
3. The time delay can be modeled by

$$\underline{y}(t) = M\,\underline{x}\,(t-T) + v_m(t-T) \tag{35}$$

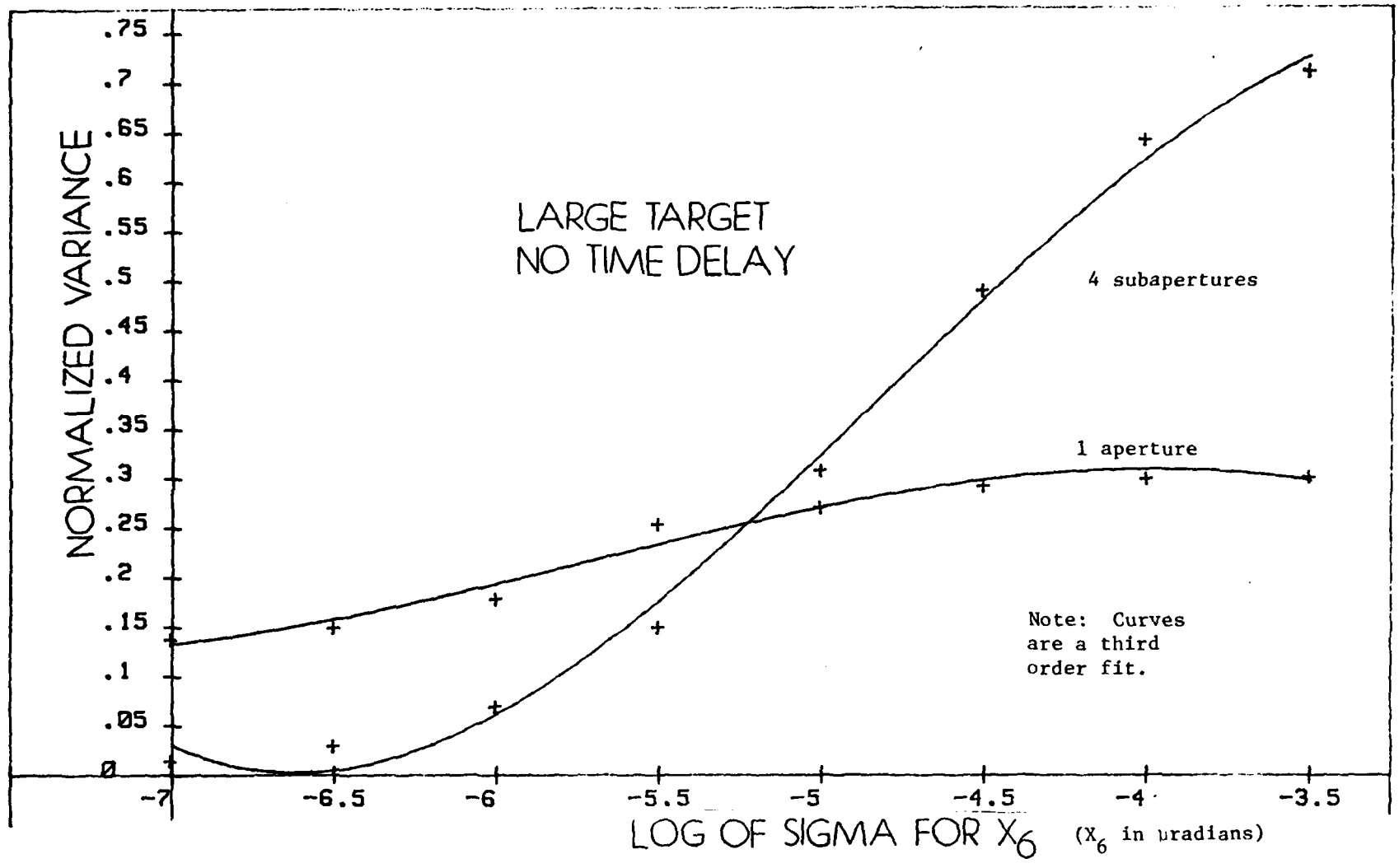

Figure 2. Normalized Variance for Large Target, No Delay.

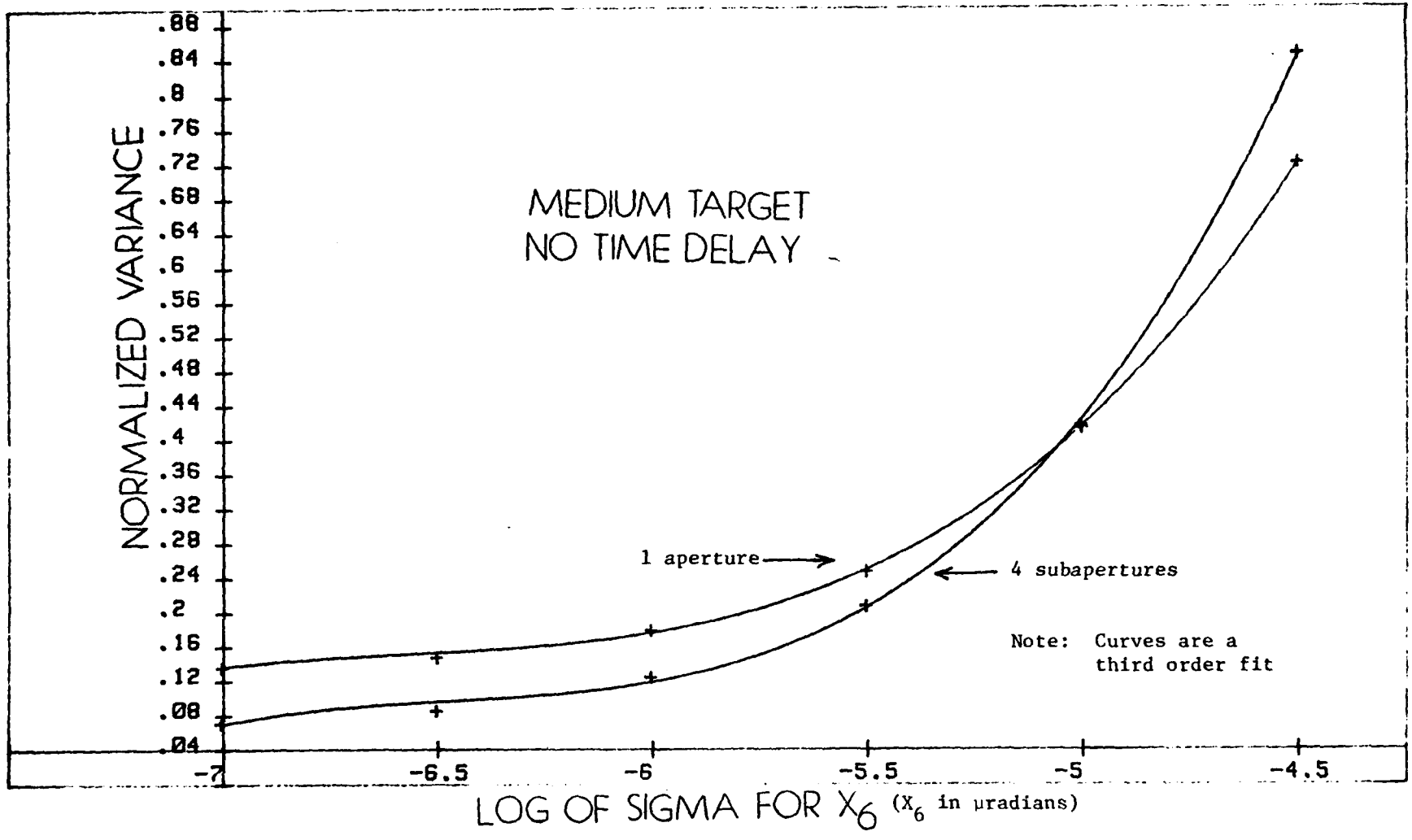

Figure 3. Normalized Variance for Medium Target, No Delay.

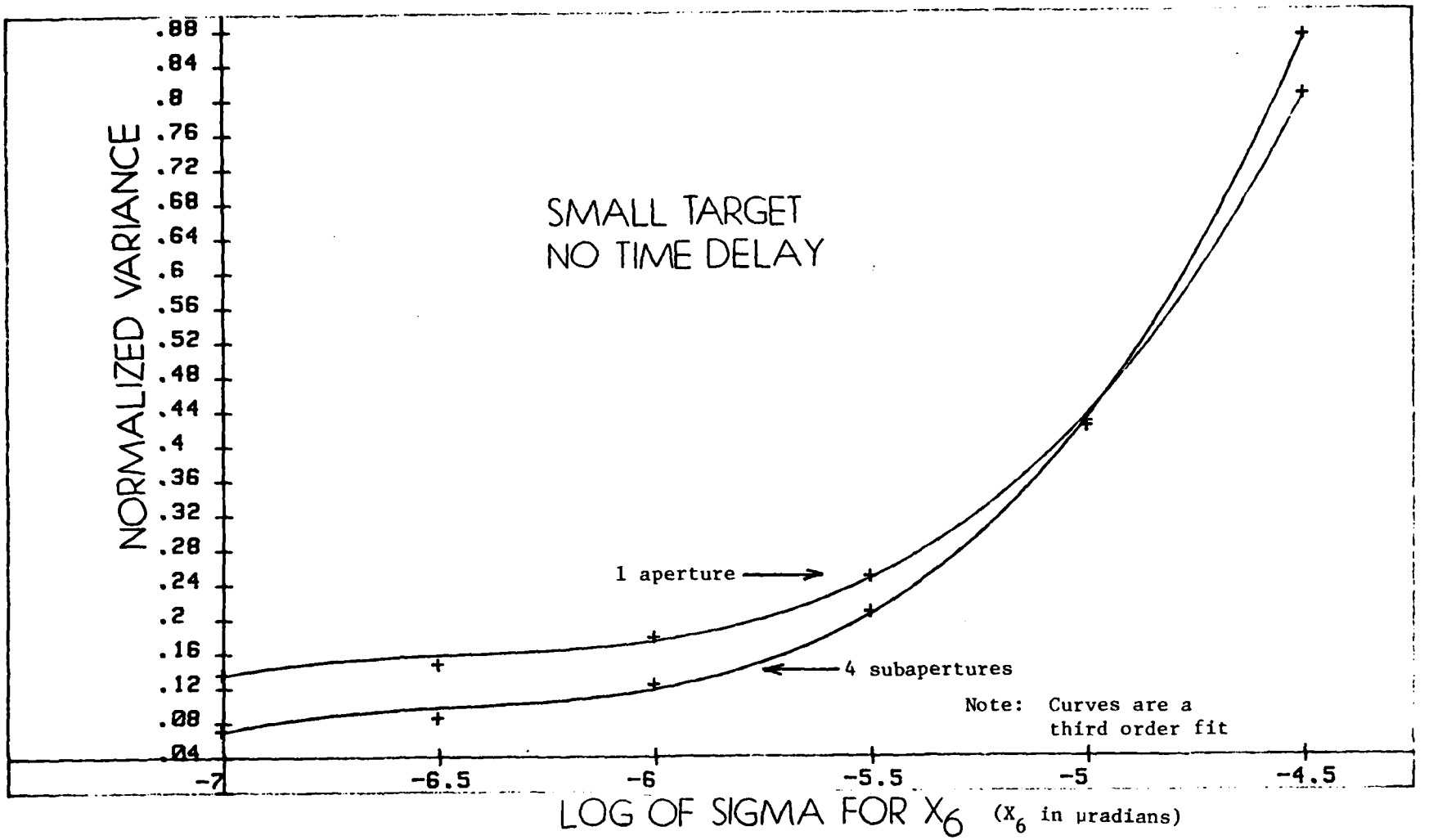

Figure 4. Normalized Variance for Small Target, No Delay.

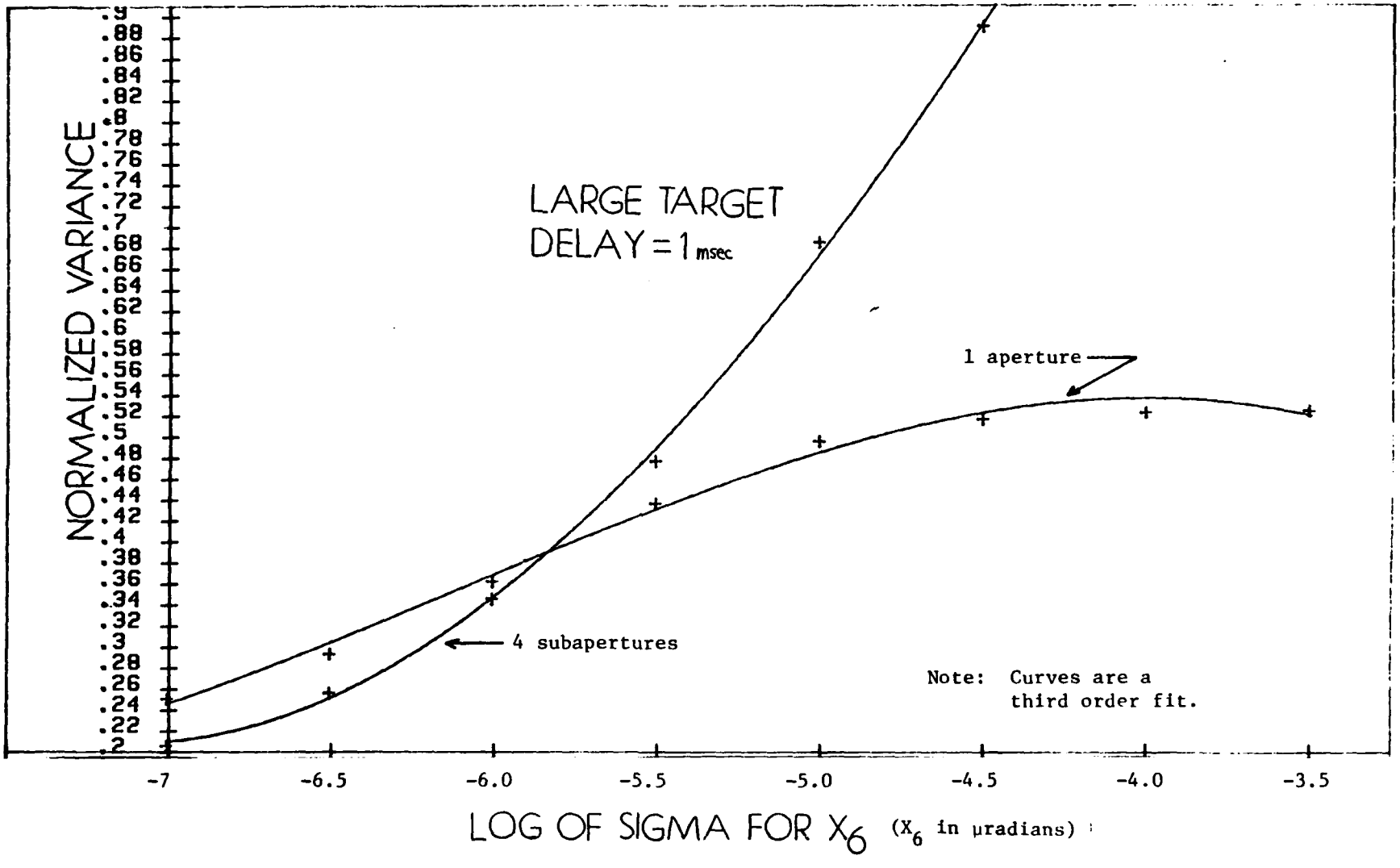

Figure 5. Normalized Variance for Large Target, Delay = 1 msec.

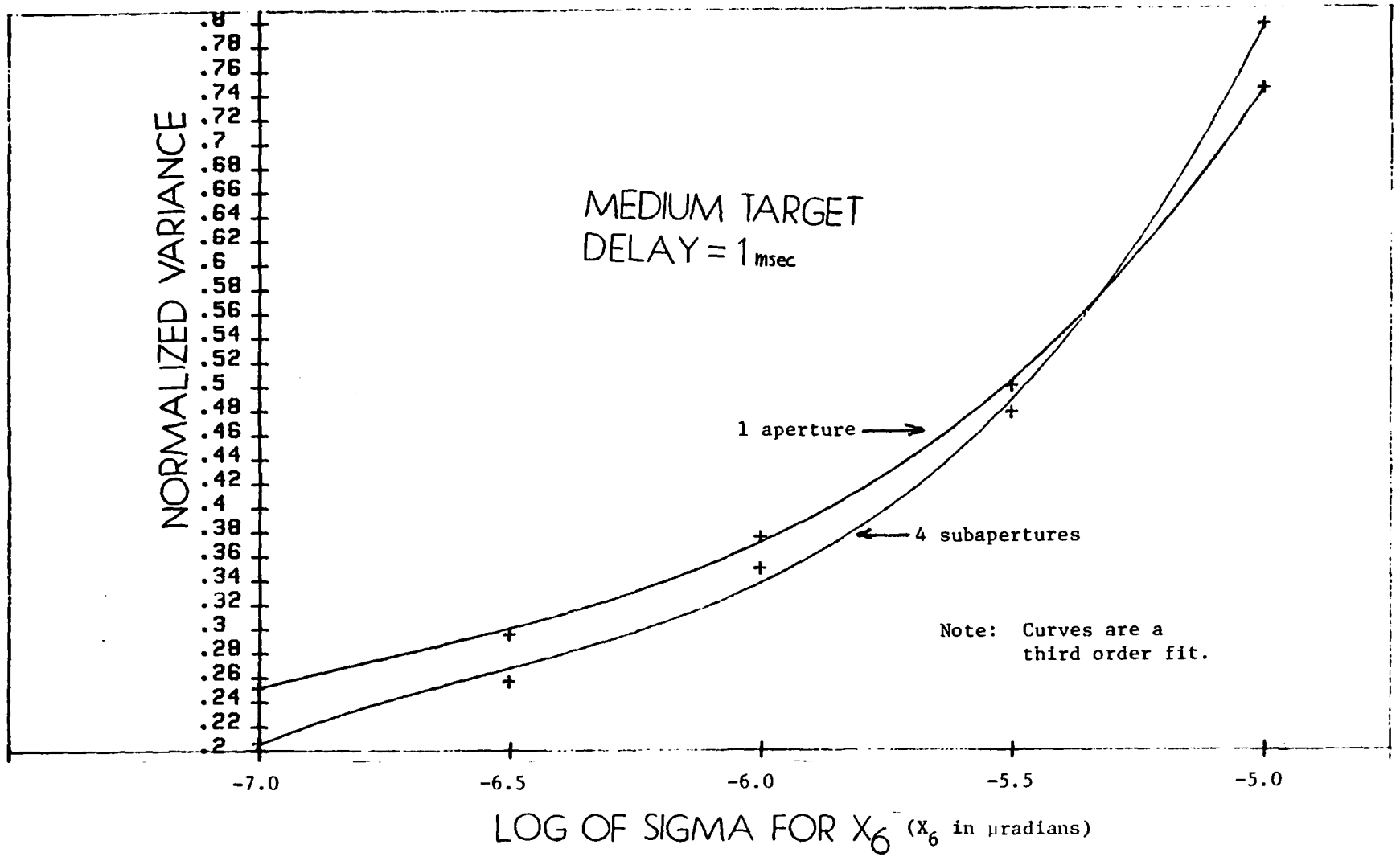

Figure 6. Normalized Variance for Medium Target, Delay = 1 msec.

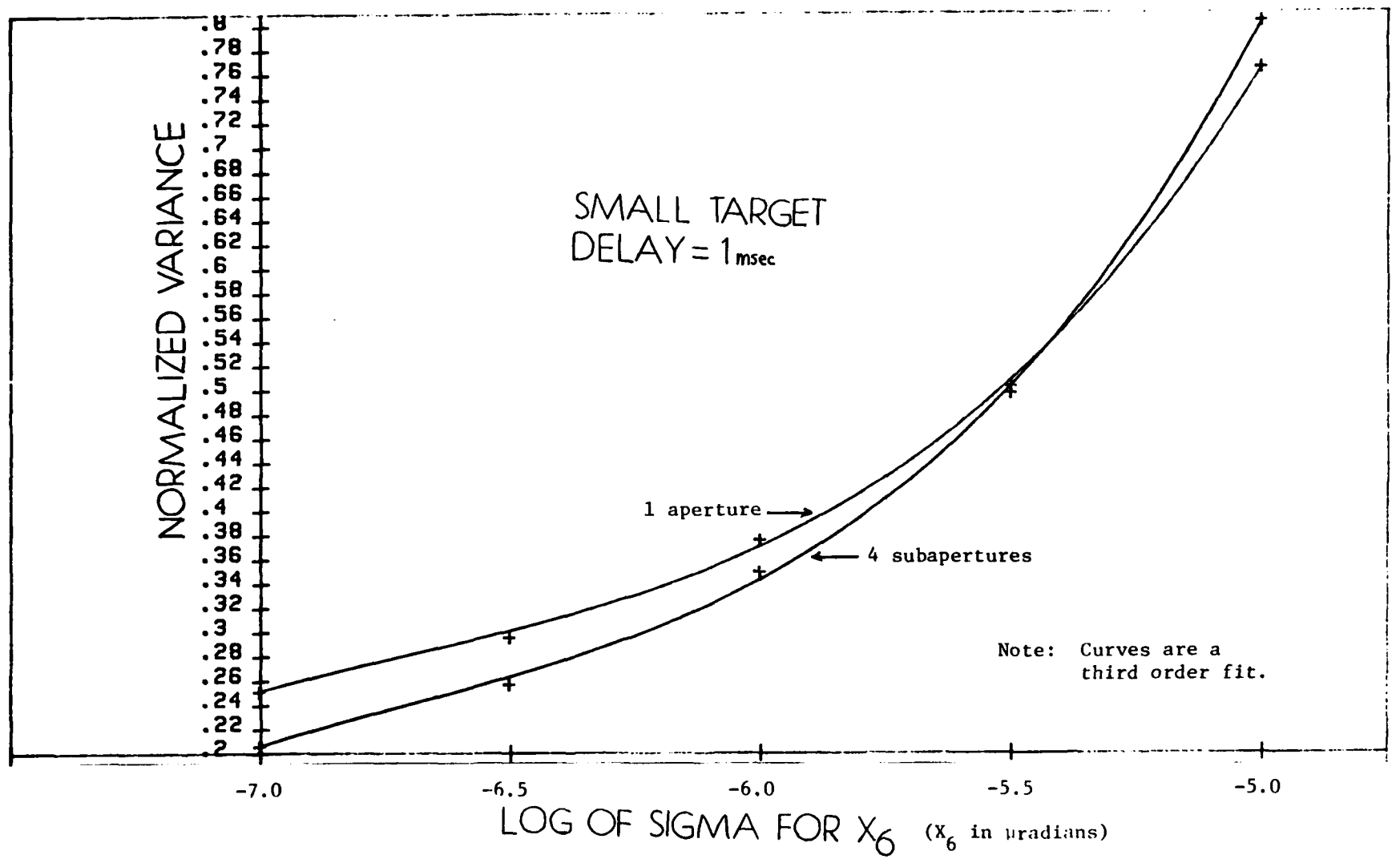

Figure 7. Normalized Variance for Small Target, Delay = 1 msec.

REFERENCES

1. D. L. Kleinman, "On an Iterative Technique for Ricatti Equation Computations," IEEE Trans. on Automatic Control, Vol AC-13, No. 1, February 1968.
2. D. L. Kleinman, "An Easy Way to Stabilize a Linear Constant System," IEEE Trans. on Automatic Control, Vol AC-15, No. 6, December 1970.
3. P. G. Smith, "Numerical Solution of the Matrix Equation $AX + X^tA^t + B = 0$," IEEE Trans. on Automatic Control, Vol AC-16, No. 3, June 1971.
4. J. H. Wilkinson and C. Peters, "Eigenvectors of Real and Complex Matrices by LR and QR Triangularizations," Numer. Math., Vol 16, pp. 181-204, 1970.
5. D. L. Kleinman, "A Description of Computer Programs Useful in Linear System Studies," AFWL Document TR-75-4, October 1975.
6. L. E. Mabius and Sol Gully, "An Optimal Control Design for the Large Pointing System," AFWL Document TR-1252-1, 12 March 1979.
7. D. P. Glasson and D. K. Guha, "Advanced Adaptive Optics Control Techniques," AFWL Document TR-78-8, January 1979.
8. B. D. O. Anderson and J. B. Moore, Linear Optimal Control, Prentice Hall, Englewood Cliffs, New Jersey, 1971.
9. Arthur Gelb (Editor), Applied Optimal Estimation, M.I.T. Press, Cambridge, Massachusetts, 1974.
10. D. L. Kleinman, "Optimal Control of Linear Systems with Time-Delay and Observation Noise," IEEE Trans. on Automatic Control, Vol. AC-14, No. 5, October 1969.
11. R. R. Butts, H. D. McIntire, and C. W. Martin, "Adaptive Optics for Laser Beam Transmission," AFWL Document.
12. C. Corsetti, AFWL Working Document.
13. R. J. Noll, "Zernike Polynomials and Atmospheric Turbulence," Journal of the Optical Society of America, Vol. 66, No. 3, March 1976.
14. J. E. Steelman, "Optimal Control of the HEL Beam," Final Report, 1980 USAF-SCEEE Summer Faculty Research Program.


FILMED
6-8